Cell Reports, Volume *23*

Supplemental Information

Mitoregulin: A lncRNA-Encoded Microprotein that Supports Mitochondrial Supercomplexes and Respiratory Efficiency

Colleen S. Stein, Pooja Jadiya, Xiaoming Zhang, Jared M. McLendon, Gabrielle M. Abouassaly, Nathan H. Witmer, Ethan J. Anderson, John W. Elrod, and Ryan L. Boudreau

SUPPLEMENTAL INFORMATION

Mitoregulin: a lncRNA-encoded microprotein that supports mitochondrial supercomplexes and respiratory efficiency

Colleen S. Stein, Pooja Jadiya, Xiaoming Zhang, Jared M. McLendon, Gabrielle M. Abouassaly, Nathan H. Witmer, Ethan J. Anderson, John W. Elrod, and Ryan L. Boudreau*

Supplemental information inventory:

Figure S1	Generation of LINC00116 (NC116) homolog (1500011K16Rik) knockout mice. Related to Figure 2 and Figure 5.
Figure S2	Intracellular localization of FLAG-tagged Mtln proteins. Related to Figure 2.
Figure S3	Metabolic phenotyping data from HeLa cells overexpressing Mtln. Related to Figure 3.
Figure S4	Mitochondrial DNA and cardiolipin content in Mtln-overexpressing HeLa cells and Mtln-KO mouse muscle tissues. Related to Figures 2-5.
Figure S5	Exercise tolerance testing and myofiber respiration measures in wild-type and Mtln-KO mice. Related to Figure 5.
Figure S6	Evaluation of oxidative stress readouts in wild-type and Mtln-KO mouse muscle tissues. Related to Figure 5.
Figure S7	Respiratory chain complex levels and Mtln distribution in wild-type and Mtln-KO mouse heart and skeletal muscle tissues. Related to Figure 5.
Figure S8	Complex I in-gel activity assay on wild-type and Mtln-KO muscle tissues. Related to Figure 5.
Figure S9	Expression of TCA and FAO pathway enzymes in wild-type and Mtln-KO mouse hearts. Related to Figure 5.
Table S1	Top genes co-expressed with human *LINC00116* and mouse *15000iiK16Rik.* Related to Figure 1.
Table S2	Gene ontology enrichment analysis on overlapping human and mouse LINC00116 co-expressed genes Related to Figure 1.
Table S3	Summary and annotation of shared human and mouse *LINC00116* co-expressed genes. Related to Figure 1.
Table S4	DNA and siRNA oligonucleotide sequences

Figure S1

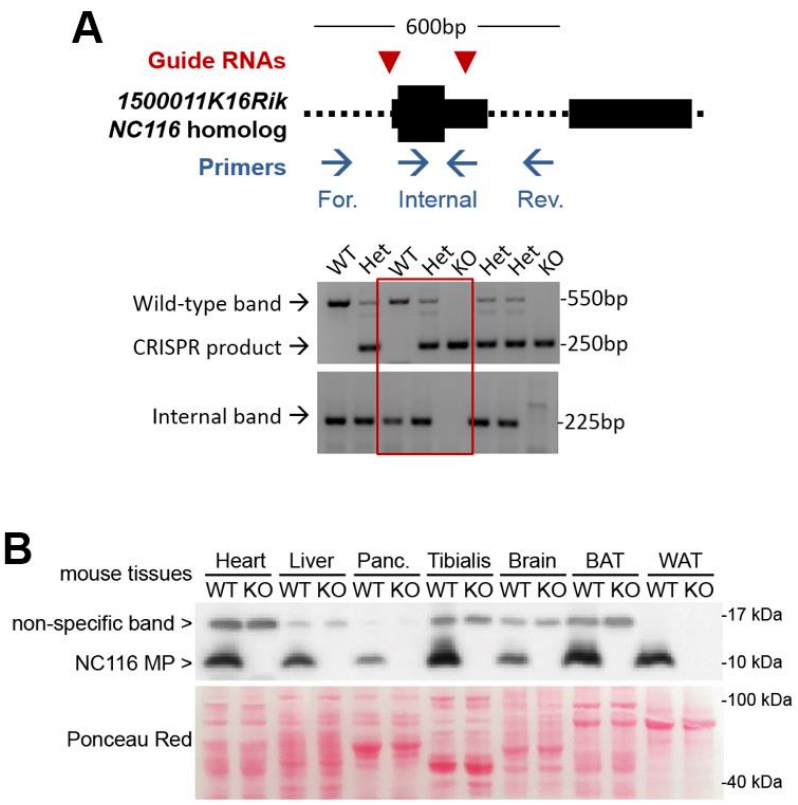

Figure S1. Generation of *LINC00116* (*NC116*) homolog (*1500011K16Rik*) knockout mice. Related to Figure 2 and Figure 5. (**A**) CRISPR/Cas9 technology was employed to delete the NC116 homolog from mouse genome using guide RNAs flanking the sORF. Genotyping primers to detect the deletion are shown in the schematic overview, and a gel image is provided to show example PCR results. (**B**) Western blot analysis on mouse tissue panels revealed a prominent 10 kDa band enriched in muscle and heart tissues that was not present in NC116-MP knockout mouse tissues. Non-specific bands and Ponceau Red serve as loading controls.

Figure S2

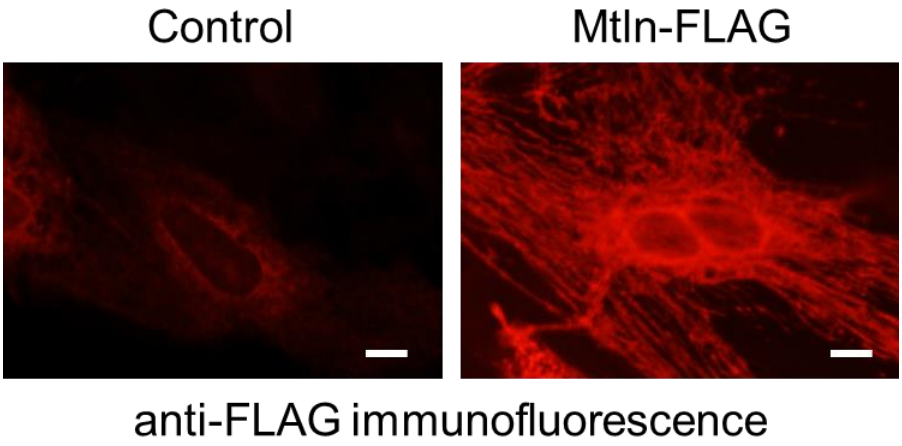

Figure S2. Intracellular localization of FLAG-tagged Mtln proteins. Related to Figure 2. C-terminal FLAG-tagged Mtln expression plasmids were transfected into cultured neonatal cardiomyocytes and immunocytochemistry was performed using an anti-FLAG antibody. Mtln-FLAG staining shows patterning consistent with mitochondrial localization; non-transfected cells serve as control. Scale bar = 10 μm.

Figure S3

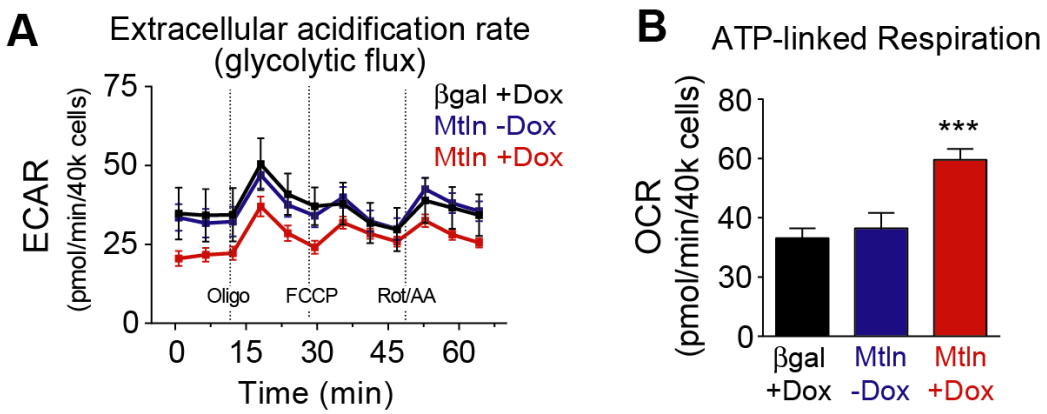

Figure S3. Metabolic phenotyping data from HeLa cells overexpressing Mtln. Related to Figure 3. Doxycycline (DOX)-inducible expression vectors were used to overexpress Mtln and beta-galactosidase (βgal, control) in cultured human HeLa cells, and 48 h later, Seahorse assays were performed in treated cells, measuring oxygen consumption (see **Figure 3C**) and extracellular acidification rates (**A**). (**B**) For oxygen consumption studies, ATP-linked respiration was calculated and plotted. Graphs are plotted as mean +/-SEM (n=12) is indicated within each bar, and p-values were determined by one-way ANOVA with Dunnett's post-hoc, comparing to βgal+Dox; ***p<0.001.

Figure S4

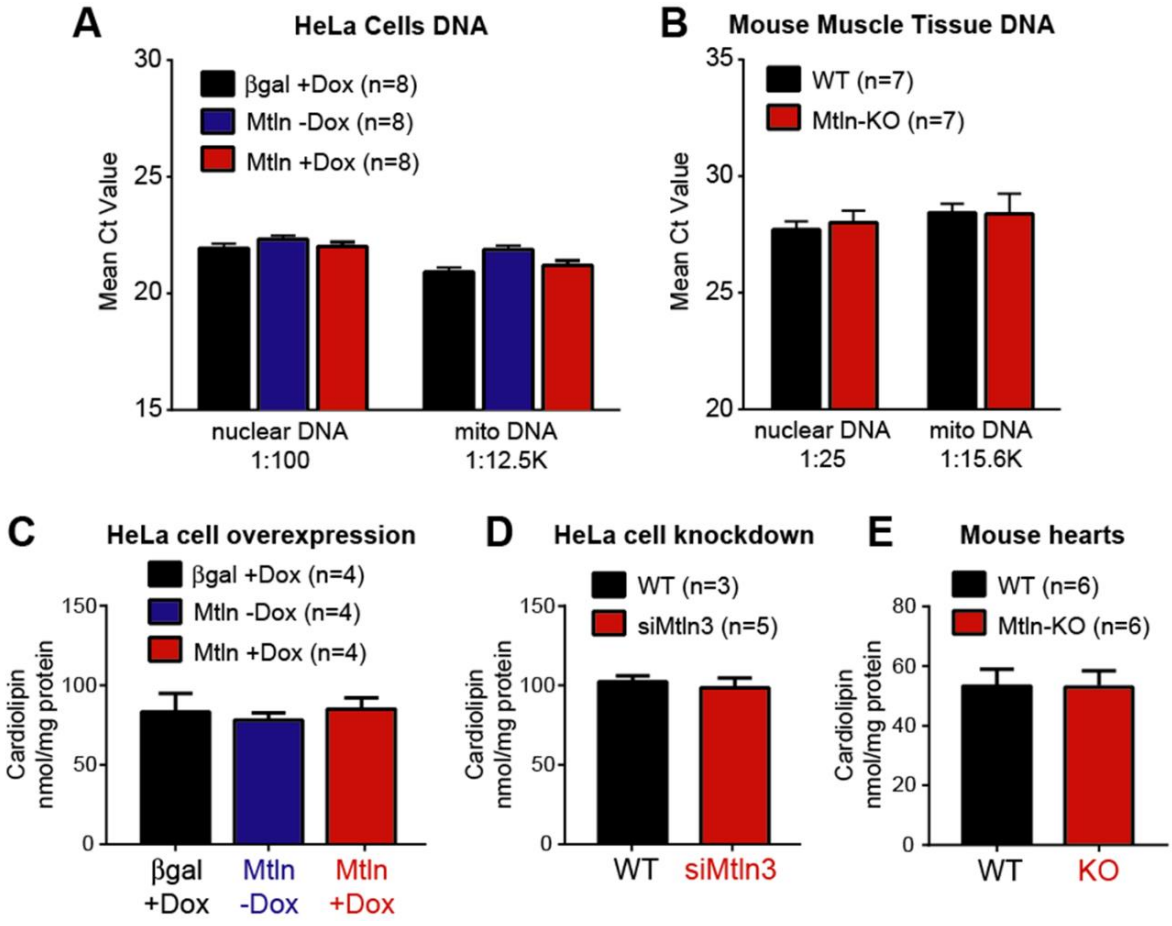

Figure S4. Mitochondrial DNA and cardiolipin content in Mtln-overexpressing HeLa cells and Mtln-KO mouse muscle tissues. Related to Figures 2-5. (**A**) Doxycycline (DOX)-inducible expression vectors were used to overexpress Mtln and beta-galactosidase (βgal, control) in cultured human HeLa cells, and 48 h later, DNA was extracted and mitochondrial and nuclear genomes quantified using QPCR (DNA dilutions indicated). (**B***) In vivo* assessment of mitochondrial and nuclear DNA levels was also performed using mouse skeletal muscle DNA samples. (**C-E**) Cardiolipin levels were measured in Dox-inducible Mtln overexpression HeLa cells (**C**), in HeLa cells with siRNA-mediated Mtln knockdown (**D**), and in wild-type (WT) and Mtln-KO mouse hearts (**E**). Graphs are plotted as mean Ct +/-SEM (sample *n* is indicated). One-way ANOVA with Dunnett's post-hoc, comparing to βgal+Dox (overexpression studies), and two-tailed t-tests (WT vs. knockdown or KO) revealed no significant differences in mitochondrial DNA levels (with or without normalization to nuclear DNA; latter not shown) nor cardiolipin levels in Mtln-overexpressing cells or Mtln-KO tissues.

Figure S5

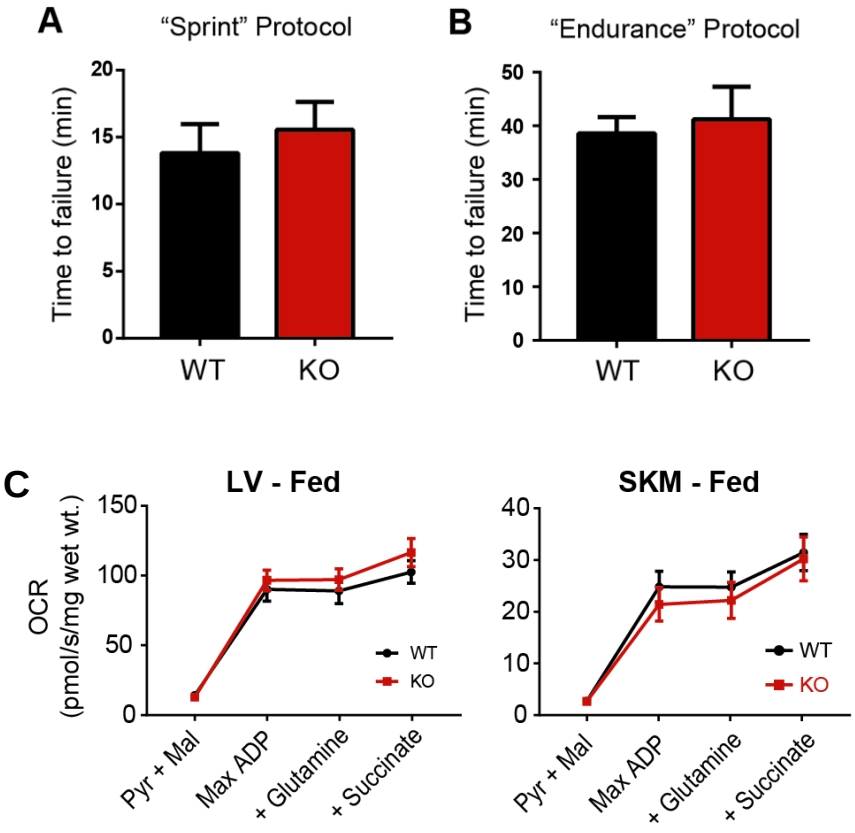

Figure S5. Exercise tolerance testing and myofiber respiration measures in wild-type and Mtln-KO mice. Related to Figure 5. Mice were subjected to exercise tolerance testing using either "sprint" (**A**) or gradual accelerated "endurance" **(B**) paradigms (see STAR Methods). Time to failure (i.e. no longer able to remain running on the treadmill) is plotted as mean +/- SEM; n=10 per genotype (5 males and 5 females for each). No significant genotype-based differences were observed; two-tailed student's t-test.(**C**) Permeabilized muscle fibers [cardiac, left ventricular (LV) and skeletal muscle (SKM), gastrocnemius)] were harvested from fed wild-type (WT) or Mtln-KO mice, and oxygen consumption rates (OCR) were measured during sequential addition of pyruvate + malate (Pyr + Mal), 1 mM ADP (Max ADP), glutamine, and succinate; data are plotted as mean +/- SEM. Fed: WT n=7 (4 males, 3 females), KO n=7 (3 males, 4 females); Fasted: n=4 females for both WT and KO.

Figure S6

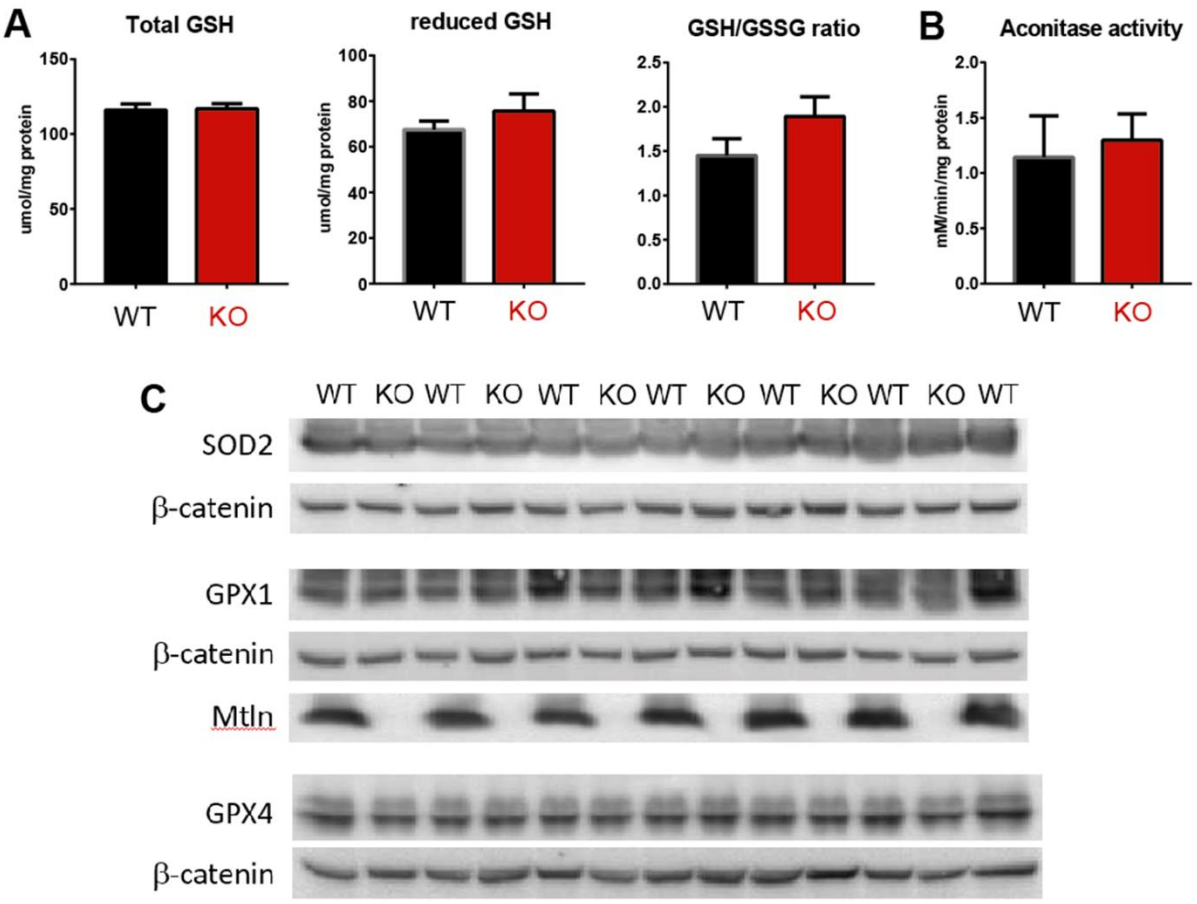

Figure S6. Evaluation of oxidative stress readouts in wild-type and Mtln-KO mouse muscle tissues. Related to Figure 5. (**A**) Levels of glutathione, both reduced (GSH) and oxidized (GSSG) forms, were measured in WT and KO mouse skeletal muscle tissue lysates. (**B**) Mitochondrial aconitase activity, which is known to be strongly suppressed by mitochondrial ROS, was measured in isolated mitochondria from WT and KO mouse hearts. Graphs are plotted as mean Ct +/-SEM (n=4 for each bar) Two-tailed t-tests revealed no significant differences between WT and Mtln-KO tissues. (**C**) Levels of key mitochondrial antioxidant enzymes (SOD2, GPX1 and GPX4) were measured in WT and KO cardiac tissues lysates, as an alternative readout for oxidative stress in the mice. No genotype-based differences were observed.

Figure S7

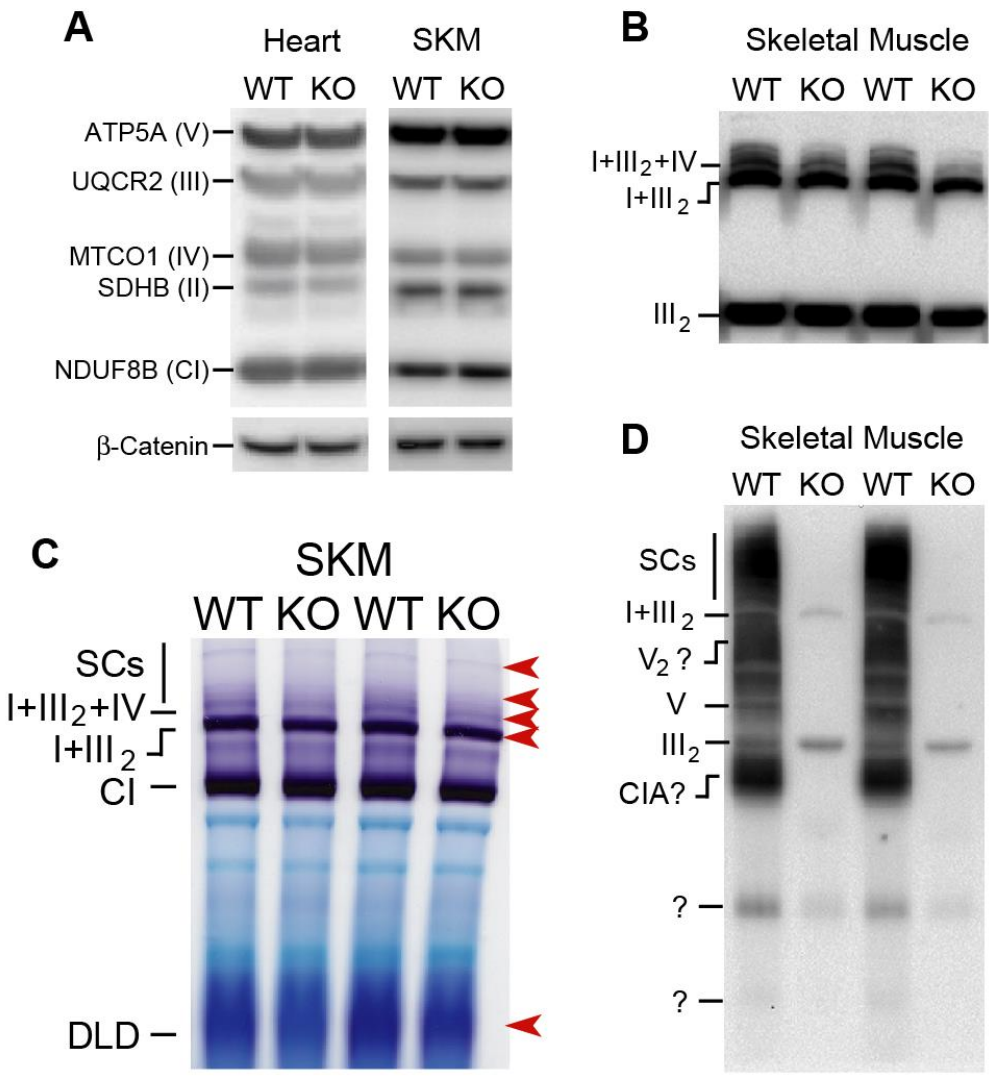

Figure S7. Respiratory chain complex levels and Mtln distribution in wild-type and Mtln-KO mouse heart and skeletal muscle tissues. Related to Figure 5. (**A**) Representative OXPHOS cocktail western blot performed on heart and skeletal muscle (SKM) tissues; n=4 per genotype were run, but no consistent genotype-based differences were observed. (**B**) Representative BN-PAGE and western blot for a Complex III subunit performed on SKM tissues. These data corroborate the reduced supercomplex formation observed in SKM by in-gel activity assay (panel **C**). (**C**) In-gel Complex I (CI) activity assay was performed on SKM tissue lysates from fed wild-type female mice (n=3/genotype, representative gels shown). Red arrows denote bands with decreased CI activity in KO mice. Upper red arrow points to a doublet band in WT hearts, with the top band virtually absent in KO mice. (**D**) Representative BN-PAGE western blot on SKM lysates shows co-migration of Mtln with various prominent mitochondrial complexes; see **Figure 5D** for cardiac tissue data.

Figure S8

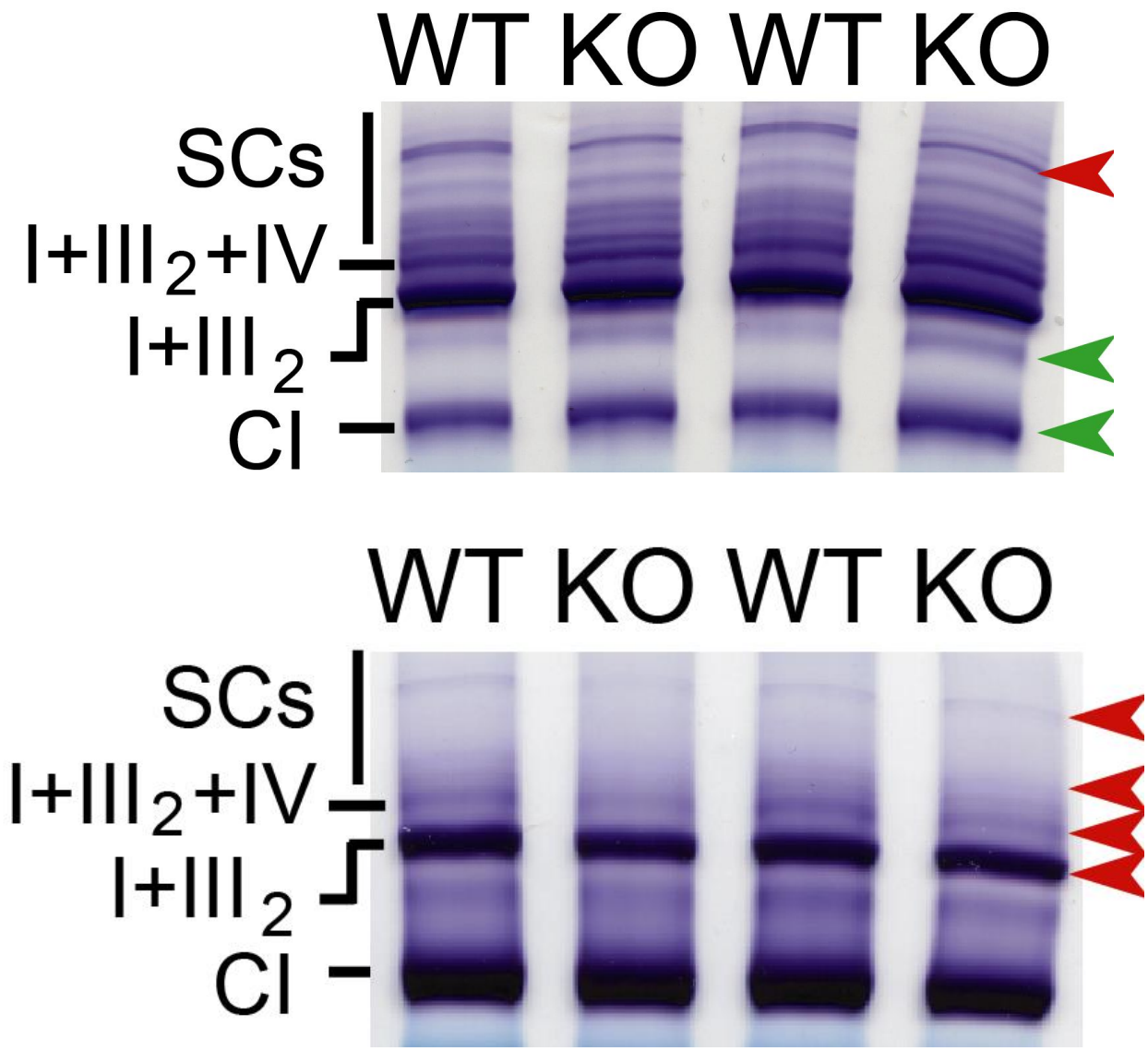

Figure S8. Complex I in-gel activity assay on wild-type and Mtln-KO muscle tissues. Related to Figure 5. Higher-power images corresponding to the Complex I (CI) in-gel activity assay presented in **Figure 5C** (heart, top) and **Figure S7C** (SKM, bottom) are provided to allow better visualization of the bands that show changes in Mtln-KO versus wild-type mice. Red and green arrows denote bands with decreased or increased (respectively) CI activity in KO mice. Upper red arrow points to a clear doublet band in WT hearts, with the top band being virtually absent in KO mice.

Figure S9

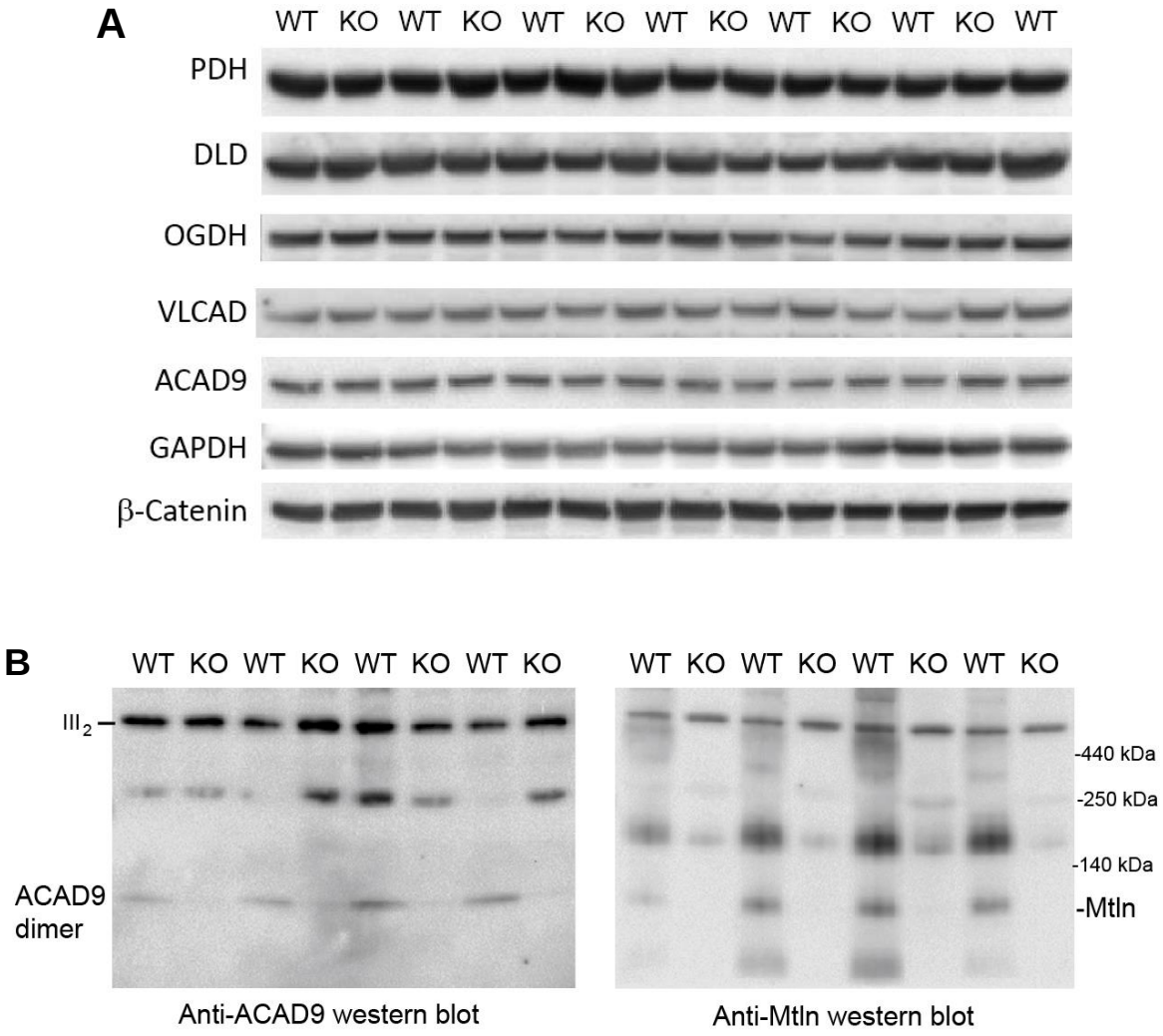

Figure S9. Expression of TCA and FAO pathway enzymes in wild-type and Mtln-KO mouse hearts. Related to Figure 5. (A) Western blot analyses performed on whole-tissue lysates from mouse hearts for the indicted proteins, which all appear to be expressed at similar levels in WT and KO mice. **(B)** BN-PAGE western blots for ACAD9 and Mtln in isolated mitochondrial show apparent loss of ACAD9 dimers in Mtln-KO mice; the dimers appear to co-migrate with Mtln containing complexes. Note: the anti-rabbit secondary antibody cross-reacts with a complex III subunit.